We obtained informed consent from all individuals and approval from the Ethics Committee at Hokkaido University Graduate School of Medicine for molecular studies. The sequences of *CGI-58* and *PNPLA2* were analyzed using the sequences in the GenBank human genome database (http://www.ncbi.nlm.nih.gov), accession numbers AI.606839 and NM020376. We amplified and sequenced the seven coding exons and exon–intron boundaries of *CGI-58/ABHD5* and the coding exons 2–10 of the ATGL gene (*PNPLA2*) with previously described primers.[1,4] Primers for amplification of exon 4 of *PNPLA2* were: forward, 5′-GACATGGGGCTATGAAGGAA-3′ and reverse, 5′-TGCCACAGCTGTTTCTTGAG-3′ The reaction products were sequenced on an ABI Prism 3100 genetic analyzer (ABI Advanced Biotechnologies, Columbia, Maryland).

The automated sequence analysis in the patient disclosed a novel homozygous duplication mutation c.475_478dupCTCC in exon 4 in the patatin domain of *PNPLA2* (Fig. 1D). This mutation was not detected in 100 control alleles from 50 unrelated healthy Japanese individuals. The patient did not show any mutations in *ABHD5/CGI-58.*

DISCUSSION

PNPLA2 encodes a lipase ATGL activated by CGI-58,[10] which plays a major role in the degradation of cytoplasmic triglycerides.[15] Experimental suppression or knockout of *PNPLA2* or its orthologs leads to cytoplasmic accumulation of triglycerides in a variety of species.[5–9,12,13,16] Furthermore, inhibition of ATGL expression using short interfering RNA (siRNA) confirmed the role of the ATGL gene in triglyceride degradation.[4]

The N-terminal region of *PNPLA2* contains a patatin domain (Fig. 1E) characteristic of a large family of storage proteins and lipid acyl hydrolases in eukaryotes and bacteria.[15] The patatin domain (PFAM accession PF01734; amino acids 10–179) is conserved in members of the *PNPLA* family[14] and in diverse species.[4] The N-terminal region of *PNPLA2* also contains a GXSXG consensus sequence for serine lipases (including the putatively active Ser47) and an α/β-hydrolase fold domain. The C-terminal region contains a hydrophobic, putative lipid-binding domain.[15]

All of the four distinct mutations in three patients having NLSD with mild myopathy reported previously were downstream of the patatin domain and none of the mutations altered the highly conserved patatin domain.[4] In these three patients the intact N-terminal region containing the catalytic site may retain lipase activity, explaining the mild myopathy, although the C-terminal region, including the hydrophobic, putative lipid binding domain, was severely altered or deleted.[4]

The present report is the second report of *PNPLA2* mutation and the *PNPLA2* mutation in our case directly affected the patatin domain. The duplication mutation in the present patient leads to a frameshift at amino acid position 160Gln, resulting in a premature termination codon 19 codons downstream (amino acid position 178) and was designated p.Gln160ProfsX19 (Fig. 1E). The peptide produced from the mutant allele has only one third the length of the normal ATGL sequence and lacks 19 amino acids present in the active, patatin domain sequence (Fig. 1D). Thus, although PNPLA2 enzyme activity in cultured fibroblasts was not analyzed in the present case, we speculate that the present patient, a homozygote for this duplication mutation, has a critical deficiency in ATGL activity. This critical deficiency might explain the severe myopathy seen in the present case. Further accumulation of similar cases with detailed genetic information is needed to clarify the genotype–phenotype correlation of NLSD with myopathy due to *PNPLA2* mutations.

We thank Ms. Akari Nagasaki for technical assistance on this project. This work was supported in part by a Grant-in-Aid from the Ministry of Education, Science, Sports, and Culture of Japan to M. Akiyama (Kiban B 18390310).

REFERENCES

1. Akiyama M, Sawamura D, Nomura Y, Sugawara M, Shimizu H. Truncation of CGI-58 protein causes malformation of lamellar granules resulting in ichthyosis in Dorfman-Chanarin syndrome. J Invest Dermatol 2003;121:1029–1034.
2. Chanarin I, Patel A, Slavin G, Wills EJ, Andrews TM, Stewart G. Neutral-lipid storage disease: a new disorder of lipid metabolism. Br Med J 1975;1:553–555.
3. Dorfman ML, Hershko C, Eisenberg S, Sagher F. Ichthyosiform dermatosis with systemic lipidosis. Arch Dermatol 1974; 110:261–266.
4. Fischer J, Lefèvre C, Morava E, Mussini J-M, Laforêt P, Negre-Salvayre A, et al. The gene encoding adipose triglyceride lipase (PNPLA2) is mutated in neutral lipid storage disease with myopathy. Nat Genet 2007;39:28–30.
5. Grönke S, Mildner A, Fellert S, Tennagels N, Petry S, Muller G, et al. Brummer lipase is an evolutionary conserved fat storage regulator in Drosophila. Cell Metab 2005;1:323–330.
6. Haemmerle G, Lass A, Zimmermann R, Gorkiewicz G, Meyer C, Rozman J, et al. Defective lipolysis and altered energy metabolism in mice lacking adipose triglyceride lipase. Science 2006;312:734–737.
7. Jenkins CM, Mancuso DJ, Yan W, Sims HF, Gibson B, Gross RW. Identification, cloning, expression, and purification of three novel human calcium-independent phospholipase A2 family members possessing triacylglycerol lipase and acylglycerol transacylase activities. J Biol Chem 2004;279:48968–48975.
8. Kurat CF, Natter K, Petschnigg J, Wolinski H, Scheuringer K, Scholz H, et al. Obese yeast: triglyceride lipolysis is function-

ally conserved from mammals to yeast. J Biol Chem 2006;281: 491–500.
9. Lake AC, Sun Y, Li JL, Kim JE, Johnson JW, Li D, et al. Expression, regulation, and triglyceride hydrolase activity of Adiponutrin family members. J Lipid Res 2005;46:2477–2487.
10. Lass A, Zimmermann R, Haemmerle G, Riederer M, Schoiswohl G, Schweiger M, et al. Adipose triglyceride lipase-mediated lipolysis of cellular fat stores is activated by CGI-58 and defective in Chanarin-Dorfman syndrome. Cell Metab 2006; 3:309–319.
11. Lefèvre C, Jobard F, Caux F, Bouadjar B, Karaduman A, Heilig R, et al. Mutations in CGI-58, the gene encoding a new protein of the esterase/lipase/thioesterase subfamily, in Chanarin-Dorfman syndrome. Am J Hum Genet 2001; 69:1002–1012.
12. Smirnova E, Goldberg EB, Makarova KS, Lin L, Brown WJ, Jackson CL. ATGL has a key role in lipid droplet/adiposome degradation in mammalian cells. EMBO Rep 2006;7: 106–113.
13. Villena JA, Roy S, Sarkadi-Nagy E, Kim KH, Sul HS. Desnutrin, an adipocyte gene encoding a novel patatin domain-containing protein, is induced by fasting and glucocorticoids: ectopic expression of desnutrin increases triglyceride hydrolysis. J Biol Chem 2004;279:47066–47075.
14. Wilson PA, Gardner SD, Lambie NM, Commans SA, Crowther DJ. Characterization of the human patatin-like phospholipase family. J Lipid Res 2006;47:1940–1949.
15. Zechner R, Strauss JG, Haemmerle G, Lass A, Zimmermann R. Lipolysis: pathway under construction. Curr Opin Lipidol 2005;16:333–340.
16. Zimmermann R, Strauss JG, Haemmerle G, Schoiswohl G, Birner-Gruenberger R, Riederer M, et al. Fat mobilization in adipose tissue is promoted by adipose triglyceride lipase. Science 2004;306:1383–1386.

A Novel *GJB2* Mutation p.Asn54His in a Patient with Palmoplantar Keratoderma, Sensorineural Hearing Loss and Knuckle Pads

Journal of Investigative Dermatology advance online publication, 25 January 2007; doi:10.1038/sj.jid.5700711

TO THE EDITOR

Mutations in the *GJB2* gene encoding connexin26 are the major cause of autosomal-recessive or -dominant non-syndromic congenital sensorineural hearing loss (SNHL) (Kelsell *et al.*, 1997; Kenneson *et al.*, 2002; refer to the connexin-deafness homepage at http://davinci.crg.es/deafness/). In addition, connexin26 mutations have been identified in autosomal-dominant syndromic congenital SNHL with palmoplantar keratoderma (PPK) (Maestrini *et al.*, 1999; Richard *et al.*, 2002, 2004; Brown *et al.*, 2003; van Steensel *et al.*, 2004; Arita *et al.*, 2006). We have encountered a Japanese boy with PPK, knuckle pads and congenital SNHL and *GJB2* mutation analysis revealed a novel mutation p.Asn54His.

The patient was a 12-year-old Japanese boy with PPK, knuckle pads on the fingers and severe SNHL. He had a congenital onset of profound bilateral SNHL. At 1 year of age, he developed PPK and knuckle pads. There was no familial history of skin disorders or auditory dysfunction. At age 12, moderate PPK was seen. Knuckle pads were apparent on all his fingers (Figure 1a and b). Acneiform follicular keratotic papules were seen on his forehead and face, although these acneiform papules might just be acne. No mutilation (pseudoainhum) was seen on the fingers. Nails, hair, and teeth were normal and no leukonychia was observed. Ophthalmologic examination revealed no apparent abnormality.

The medical ethical committee at Hokkaido University approved all studies described below. The study was conducted according to the Declaration of Helsinki Principles. Participants or their legal guardian gave their written informed consent. The coding region of *GJB2* (Genbank accession no. NM 004004) was amplified from genomic DNA by PCR, as described previously (Richard *et al.*, 1998). Direct sequencing of the patient's PCR products revealed that the patient was a heterozygote for a novel missense mutation p.Asn54His (A to C substitution at nucleotide position 160: asparagine 54 (AAC) to histidine (CAC)) in *GJB2* (Figure 1d), which was not found in his mother. We were unable to obtain a DNA sample from his father. This mutation was not found in 100 normal unrelated Japanese alleles (50 normal unrelated Japanese individuals) by direct sequence analysis and was unlikely to be a polymorphism (data not shown). Direct sequencing of all the exons and exon/intron borders of *GJB2* failed to detect any other pathogenic mutation in the patient's DNA.

A skin biopsy obtained from the palmar lesion revealed orthohyperkeratosis and mild regular acanthosis. Electron microscopy of the upper epidermal keratinocytes showed normal morphology with normal keratin network and keratohyalin granules. Gap junctions existed in all living epidermal layers, and the morphology of gap junctions was normal, showing a typical pentalaminar structure, 20 nm in width (Figure 1e).

Immunofluorescent stainings with rabbit polyclonal anti-connexin26 antibody (the epitope is a portion of the cytoplasmic loop of connexin26) (ZYMED Laboratories, San Francisco, CA) showed strong connexin26 expression in the upper layers of the wide rete ridge in the patient's palmar epidermis (Figure 1f), compared with weak connexin26 expression in the normal palmar epidermis (Figure 1g). The antibody used in this study binds to both normal and mutated connexin26 peptides. Thus, it was not clear whether the overexpressed connexin26 in the patient's epidermis was normal and/or mutated. Connexin43 immunostainings with mouse monoclonal anti-connexin43 antibody (clone 4E6.2) (Chemicon International, Temecula, CA) revealed that the expression of connexin43 was almost completely membranous and appeared similar both in the patient's and normal control skin (data not shown).

Bart–Pumphrey syndrome is characterized by knuckle pads, PPK, SNHL, and leukonychia (Bart and Pumphrey, 1967). The present patient cannot be diagnosed with Bart–Pumphrey syndrome because of a lack of nail involvement. In two families which were reported as suffering from Bart–Pumphrey syndrome and harboring *GJB2* mutations, an affected patient in one family did not show any leukonychia and, in the other family, two affected family members showed leukonychia, but the other three failed to show any leukonychia (Alexandrino *et al.*, 2005; Leonard *et al.*, 2005). In this context, leukonychia is not an essential clinical feature in the patients with knuckle pad formation, PPK, and SNHL. It is questionable whether Bart–Pumphrey syndrome having leukonychia as an essential characteristic/diagnostic feature is a distinct clinical entity from the knuckle pads, PPK, and SNHL phenotype. Thus, in this study, we have adopted the clinical entity "knuckle pads, PPK, and SNHL", instead of Bart–Pumphrey syndrome.

Abbreviations: PPK, palmoplantar keratoderma; SNHL, sensorineural hearing loss

Most pathogenic *GJB2* mutations causing both SNHL and skin manifestations cluster in the first extracellular loop of the connexin26 peptide (Richard *et al.*, 1998, 2004; Maestrini *et al.*, 1999; Heathcote *et al.*, 2000; Uyguner *et al.*, 2002; Oshima *et al.*, 2003; Yotsumoto *et al.*, 2003; Montgomery *et al.*, 2004; Alexandrino *et al.*, 2005; Leonard *et al.*, 2005). This fact clearly suggests that this extracellular domain is important for the correct formation and/or function of gap junctions. Indeed, the evolutionary conserved, first extracellular loop domain was reported to play an essential role in the assembly of connexon hemichannels, connexon–connexon interactions, voltage gating, and channel permeability (Rubin *et al.*, 1992; White *et al.*, 1995; Oshima *et al.*, 2003).

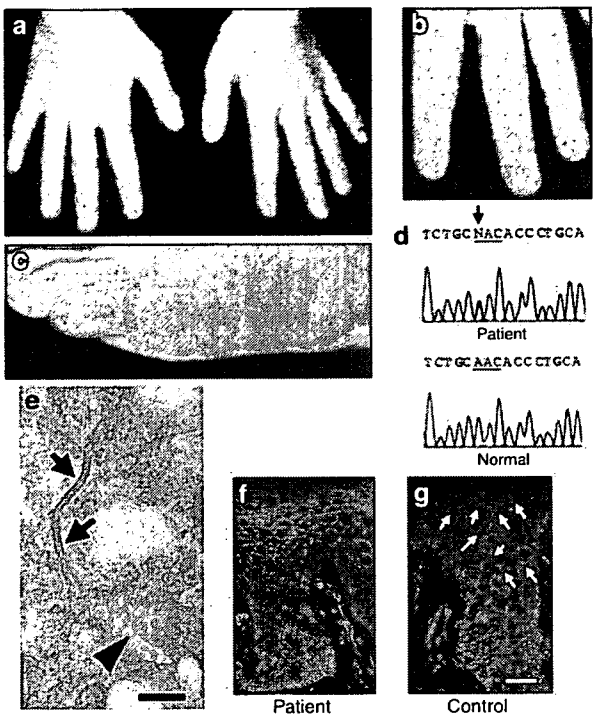

Figure 1. The patient's clinical features, *GJB2* mutation, gap junction ultrastructure and upregulated connexin26 expression. (**a–c**) The patient's clinical features at the age of 12. (**a**) Severe knuckle pads were seen over all the fingers. (**b**) The knuckle pads were sharply demarcated, hyperkeratotic plaques. (**b**) Nails were not involved. (**c**) Hyperkeratotic plaques resembling knuckle pads were seen in the toes and periphery of the foot. (**d**) Mutation in connexin26 gene (*GJB2*). A novel heterozygous A to C substitution at the codon 54 (c.160A>C) was detected in the patient's genomic DNA. This mutation leads to the amino-acid substitution, p.Asn54His. (**e**) A gap junction with normal, typical pentalaminar structure, 20 nm in width, was observed in the periphery of the keratinocyte in the lesional epidermis on the palm. Arrows, gap junction; arrowhead, desmosome. (**f**) Upregulated connexin26 expression was seen in the spinous layers of the patient's lesional skin in the palm. (**g**) In the normal control palmar skin, weak connexin26 immunostaining (green) was observed in the spinous layers (white arrows). Connexin26 immunostaining, green (FITC); nuclear staining, red (propidium iodide). (**e**) Bar = 100 nm and (**g**) 50 μm.

The causative *GJB2* missense mutations in the previously reported three families showing knuckle pads, PPK, and SNHL were a replacement of glycine 59 in two families (Alexandrino et al., 2005; Leonard *et al.*, 2005) and a replacement of asparagine 54 in the other family (Richard *et al.*, 2004), both in the evolutionary conserved first extracellular loop of connexin26. In the present case, the *GJB2* mutation similarly lay in the asparagine 54 residue. Asparagine was replaced by histidine in the present case and by lysine in the previously reported Bart–Pumphrey syndrome family (Richard *et al.*, 2004). Asparagine is an acidic amino acid and histidine and lysine are basic amino acids. Thus, the amino-acid exchange would probably result in an altered electron charge at the mutation site and may lead to defective voltage gating affecting the formation and function of gap junctions. In addition, histidine has a relatively large, aromatic side chain, and the amino-acid change may lead to a conforma-

Table 1. Mutations within the first extracellular domain of connexin26 and associated clinical features

Syndromes	KID syndrome		Knuckle pads, PPK, and SNHL			VWS	PPK and SNHL	
Causative mutations	p.Ala40Val	p.Asp50Asn/Tyr	p.Asn54Lys	p.Asn54His[1]	p.Gly59Arg/Ser	p.Asp66His	p.Gly59Ala	p.Arg75Trp/Gln
Knuckle pads	–	–	+	+	+	–	–	–
PPK	+	+	+	+	+	+	+	+
SNHL	+	+	+	+	+	+	+	+
Nail dystrophy (leukonychia)	+	+	±	–	–	–	–	–
Keratitis	+	+	–	–	–	–	–	–
Pseudoainhum	–	–	–	–	–	+	–	–

KID, keratitis–ichthyosis–deafness; PPK, palmoplantar keratosis; SNHL, sensorineural hearing loss; VWS, Vohwinkel syndrome; +, observed; –, not observed or not described; ±, observed in some case, but not in the others.
[1]Present case.

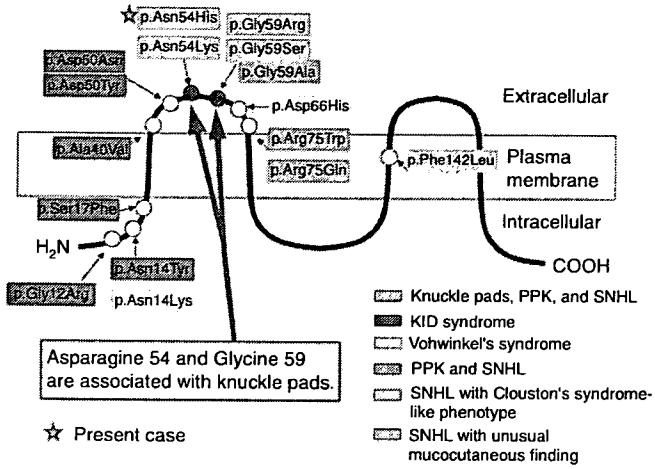

Figure 2. Connexin26 molecular structure, mutations and their associated skin syndromes. Connexin26 gene (*GJB2*) mutations associated with syndromic SNHL cluster in the N-terminal portion of connexin26, mainly in the first extracellular loop. Note all the mutations associated with knuckle pads affect asparagines 54 or glycine 59. Asterisk represents the present case.

tional change of the first extracellular domain in the present case. To determine the effect of this mutation on cell–cell gap junction function, functional studies by expressing the mutant allele in cultured cells are necessary.

Among the mutations located in the first extracellular loop of connexin26, differences in the site and nature of the mutations are thought to lead to the distinctive clinical phenotypes, as shown in Table 1 and Figure 2. These data including our case suggest that alterations of the amino-acid residues asparagines 54 and glycine 59 in the central portion of the first extracellular loop might be associated with the clinical knuckle pad feature, although we do not have any direct evidence to support that the mutations caused knuckle pads. Further accumulation of the similar cases should be needed to conclude this mutation lead to knuckle pads.

CONFLICT OF INTEREST

The authors state no conflict of interest.

ACKNOWLEDGMENTS

We thank the patient and his family for their generous cooperation and Ms Akari Nagasaki and Ms Satoko Ishikawa for their fine technical assistance on this project. This work was supported in part by Grant-in-Aid from the Ministry of Education, Science, Sports, and Culture of Japan to M. Akiyama (Kiban B 18390310).

Masashi Akiyama[1], Kaori Sakai[1], Ken Arita[1], Yukiko Nomura[1], Kei Ito[1], Kazuo Kodama[1], James R. McMillan[1], Kinuko Kobayashi[2], Daisuke Sawamura[1] and Hiroshi Shimizu[1]

[1]Department of Dermatology, Hokkaido University Graduate School of Medicine, Sapporo, Japan and [2]Kobayashi Skin Clinic, Sapporo, Japan
E-mail: akiyama@med.hokudai.ac.jp

REFERENCES

Alexandrino F, Sartorato EL, Marques-de-Faria AP, Steiner CE (2005) G59S mutation in the *GJB2* (connexin 26) gene in a patient with Bart–Pumphrey syndrome. *Am J Med Genet* 136A:282–4

Arita K, Akiyama M, Aizawa T, Umetsu Y, Segawa I, Goto M *et al.* (2006) A novel N14Y mutation in connexin26 in KID syndrome – analyses of altered gap junctional communication and molecular structure of N-terminus of mutated connexin26. *Am J Pathol* 169: 416–23

Bart RS, Pumphrey RE (1967) Knuckle pads, leukonychia and deafness – a dominant inherited syndrome. *New Engl J Med* 276:202–7

Brown CW, Levy ML, Flaitz CM, Reid BS, Manolidis S, Hebert AA *et al.* (2003) A novel GJB2 (connexin 26) mutation, F142L, in a patient with unusual mucocutaneous findings and deafness. *J Invest Dermatol* 121:1221–3

Heathcote K, Syrris P, Carter ND, Patton MA (2000) A connexin 26 mutation causes a syndrome of sensorineural hearing loss and palmoplantar hyperkeratosis (MIM 148350). *J Med Genet* 37:50–1

Kelsell DP, Dunlop J, Stevens HP, Lench NJ, Liang JN, Parry G *et al.* (1997) Connexin 26 mutations in hereditary non-syndromic sensorineural deafness. *Nature* 387:80–3

Kenneson A, Van Naarden Braun K, Boyle C (2002) GJB2 (connexin 26) variants and nonsyndromic sensorineural hearing loss: a HuGE review. *Genet Med* 4:258–74

Leonard NJ, Krol AL, Bleoo S, Somerville MJ (2005) Sensorineural hearing loss, striate palmoplantar hyperkeratosis, and knuckle pads in a patient with a novel connexin 26 (GJB2) mutation. *J Med Genet* 42:e2

Maestrini E, Korge BP, Ocana-Sierra J, Calzolari E, Cambiaghi S, Scudder PM *et al.* (1999) A missense mutation in connexin26, D66H, causes mutilating keratodermawith sensorineural deafness (Vohwinkel's syndrome) in three unrelated families. *Hum Mol Genet* 8:1237–43

Montgomery JR, White TW, Martin BL, Turner ML, Holland SM (2004) A novel connexin 26 gene mutation associated with features of the keratitis–ichthyosis–deafness syndrome and the follicular occlusion triad. *J Am Acad Dermatol* 51:377–82

Oshima A, Doi T, Mitsuoka K, Maeda S, Fujiyoshi Y (2003) Roles of M34, C64, and R75 in the assembly of human connexin 26: implication for key amino acid residues for channel formation and function. *J Biol Chem* 278:1807–16

Richard G, Brown N, Ishida-Yamamoto A, Krol A (2004) Expanding the phenotypic spectrum of Cx26 disorders: Bart–Pumphrey syndrome is caused by a novel missense mutation in GJB2. *J Invest Dermatol* 123: 856–63

Richard G, Rouan F, Willoughby CE, Brown N, Chung P, Ryynanen M *et al.* (2002) Missense mutations in GJB2 encoding connexin-26 cause the ectodermal dysplasia keratitis–ichthyosis–deafness syndrome. *Am J Hum Genet* 70:1341–8

Richard G, White TW, Smith LE, Bailey RA, Compton JG, Paul DL *et al.* (1998) Functional defects of Cx26 resulting from a heterozygous missense mutation in a family with dominant deaf-mutism and palmoplantar keratoderma. *Hum Genet* 103:393–9

Rubin JB, Verselis VK, Bennett MV, Bargiello TA (1992) Molecular analysis of voltage dependence of heterotypic gap junctions formed by connexins 26 and 32. *Biophys J* 62:183–93

Uyguner O, Tukel T, Baykal C, Eris H, Emiroglu M, Hafiz G *et al.* (2002) The novel R75Q mutation in the GJB2 gene causes autosomal dominant hearing loss and palmoplantar keratoderma in a Turkish family. *Clin Genet* 62:306–9

van Steensel MA, Steijlen PM, Bladergroen RS, Hoefsloot EH, Ravenswaaij-Arts CM, van Geel M (2004) A phenotype resembling the Clouston syndrome with deafness is associated with a novel missense GJB2 mutation. *J Invest Dermatol* 123:291–3

White TW, Paul DL, Goodenough DA, Bruzzone R (1995) Functional analysis of selective interactions among rodent connexins. *Mol Biol Cell* 6:459–70

Yotsumoto S, Hashiguchi T, Chen X, Ohtake N, Tomitaka A, Akamatsu H *et al.* (2003) Novel mutations in GJB2 encoding connexin-26 in Japanese patients with keratitis–ichthyosis–deafness syndrome. *Br J Dermatol* 148: 649–53

doi: 10.1111/j.1365-2230.2007.02542.x

Extensive proliferative nodules in a case of giant congenital naevus

S. Aoyagi, M. Akiyama, M. Mashiko, A. Shibaki and H. Shimizu

Department of Dermatology, Hokkaido University Graduate School of Medicine, Sapporo, Japan

Summary

The rare presence of proliferative nodules in cases of giant congenital naevus can, in some cases, be potentially misdiagnosed as neonatal melanoma. We report here a case of multiple, proliferative nodules found in a giant congenital naevus lesion in a female neonatal patient diagnosed with neurocutaneous melanosis. Our initial clinical observations of this case suggested the possibility of primary cutaneous neonatal melanoma or skin metastasis from a melanoma in the meninges or elsewhere in the central nervous system. However, histological examination revealed no sign of melanoma, abnormal mitosis, necrosis or any malignant change. Pagetoid arrays of naevus cells in the junctional zone and myxoid changes present in a significant portion of the dermis led to the diagnosis of proliferative nodules. Distinct histological patterns seen in the proliferative nodules in our neonatal patient were useful to differentiate between benign pigmented nodular lesions in a giant congenital naevus and malignant melanoma, and reduced the chance of misdiagnosis.

Since the first descriptions in the 1990s of proliferative nodules in congenital naevi as 'proliferative dermal lesions in congenital naevi' by Elder and Murphy,[1] or as 'atypical dermal melanocytic proliferations' by Clark *et al.*,[2] additional cases of 'proliferative nodules'[3–8] have been reported in congenital naevi. These nodules generally occur within a giant-type congenital naevus present since birth.[3] The surface generally appears smooth and shiny, black or dark-brown in colour and often ulcerated. Such features make these proliferative nodules difficult to differentiate clinically from malignant melanoma.[5] We report a case of extraordinarily extensive proliferative nodules that developed in a giant congenital naevus from neurocutaneous melanosis and discuss the clinical and histological features that help to differentiate proliferative nodules from malignant melanoma.

Correspondence: Dr Satoru Aoyagi, MD, Department of Dermatology, Hokkaido University Graduate School of Medicine, N15 W7, Kita-ku, Sapporo 060-8638, Japan.
E-mail: saoyagi@med.hokudai.ac.jp

Conflict of interest: none declared.

Accepted for publication 7 May 2007

Figure 1 Large, clustered proliferative nodules within the giant congenital naevus of the bathing-suit type with multiple satellite naevi.

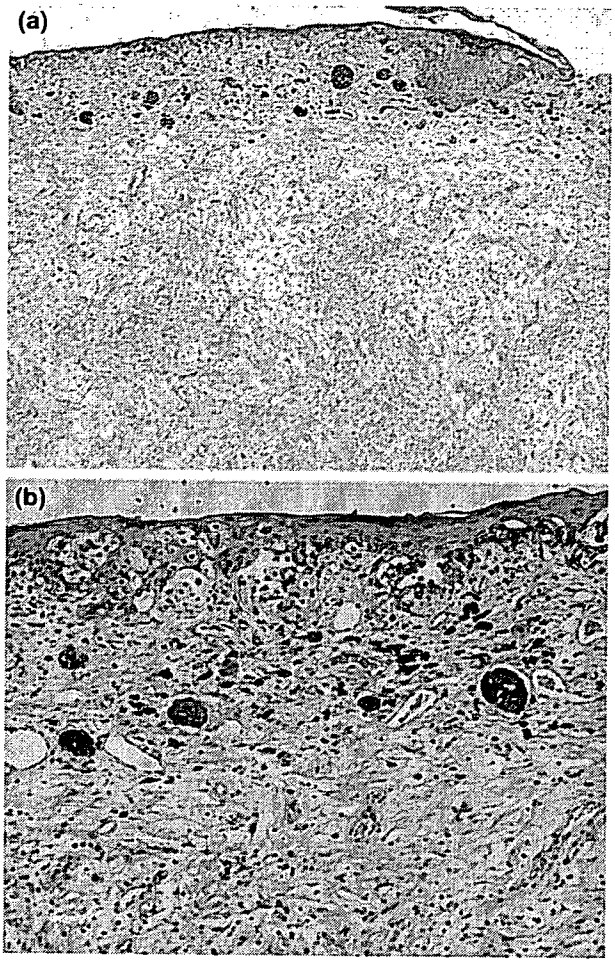

Figure 2 (a) Tumour cell nests were observed in the junctional zone and throughout the dermis; (b) pagetoid arrays of naevus cells were seen in the junctional zone. Haematoxylin and eosin, original magnification (a) ×100; (b) ×200.

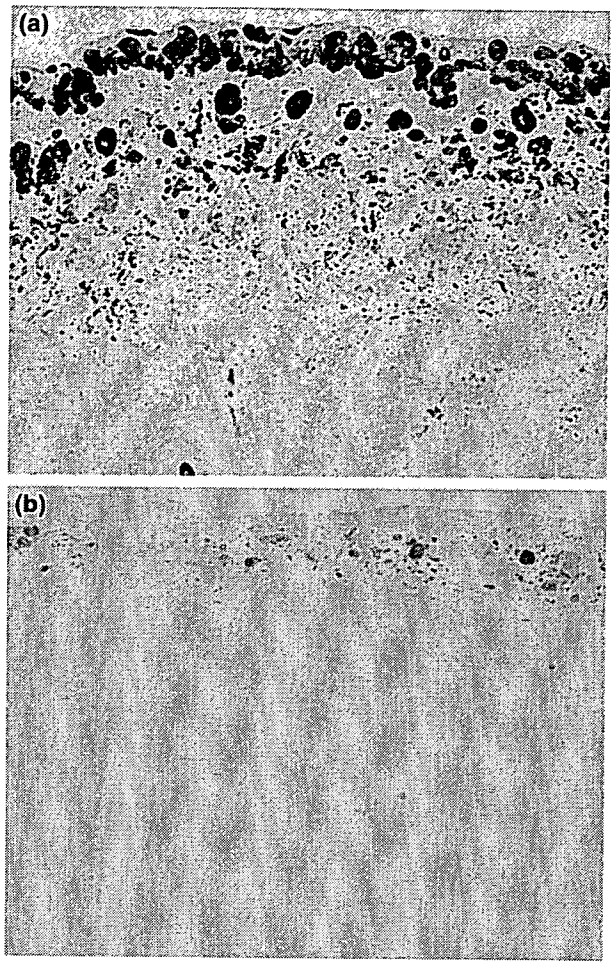

Figure 3 HMB-45 and alcian blue staining of the proliferative nodule. (a) The tumour cells in the junctional zone and the upper dermis positively stained with anti-HMB45 antibody (original magnification ×200). (b) Large portions of the dermis were positive for alcian blue stain at pH 2.5 (original magnification ×200).

Report

The patient was a full-term Japanese girl with no known family history of hereditary skin disorders. On physical examination, we observed a giant naevus of the 'bathing-suit' type, along with multiple satellite naevi on the head, face and limbs, all of which had been present since birth (Fig. 1a). Approximately 20 black, smooth and elastic proliferative nodules, up to 35 mm in diameter, were seen in the giant congenital naevi, especially over the lower abdomen and genitals, where several large, darker proliferative nodules were clustered (Fig. 1b).

At 2 months of age, the patient underwent various diagnostic examinations, including medullar magnetic resonance imaging (MRI), a radiographic study of the vertebral column and brain echography. From the MRI scan, we detected the presence of melanosis in the cerebellum, but no evidence of malignant melanoma. Results of neurological examinations were normal.

Excisional biopsy of one of the large darker nodules in the lower abdomen was performed for histological analysis. Histological examination showed a proliferation of melanocytes extending from the junctional zone throughout the dermis, into subcutaneous fat tissue (Fig. 2a). Nests of melanocytes with a pale cytoplasm and monomorphous nuclei were situated at the junction (Fig. 2b). These cells were positive for HMB-45 (Dako Cytomation, Kyoto, Japan) (Fig. 3a). Clusters of plump, oval melanocytes with intense pigmentation and large vesicular nuclei were located in the papillary dermis. These melanocytes gradually matured into small, round cells in certain areas. Large portions of the dermis were

also occupied by myxoid connective tissues, identified by staining with alcian blue at pH 2.5 (Fig. 3b). Notably, mitoses and necrotic foci were not present. Hence, the observed histological characteristics were consistent with proliferative nodules associated with a congenital naevus.

The naevoid lesions and nodules were partially ablated and excised over the course of several surgical operations over 6 months. Other nodules within the congenital naevus resolved spontaneously over 2 years. At 3 years of age, the child remained in good health with no evidence of malignancy.

Proliferative nodules within a giant congenital naevus are relatively rare. To differentiate these nodules from melanoma, Elder and Elenitsas[9] describe several characteristics that indicate their benign course: (i) evidence of maturation, such as blending or transitional forms between nodular and naevus cells, (ii) a low mitotic rate, and (iii) lack of necrosis within the nodule or high-grade uniform cellular atypia.

Although ulcerations in melanocytic lesions are generally indicative of their malignant nature, neonatal or congenital erosions in giant congenital naevi are not regarded as malignant features. The skin of newborns is more fragile than that of children and adults. Thus, ulcerations and erosions on proliferative nodules are likely to be due to friction or trauma to the epidermis overlying the naevus during birth.[10]

In this patient, both necrosis and cellular atypia were absent, and few mitotic cells were detected during histological examination. In addition, cellular maturation was seen in some areas. These findings suggested that the nodules in this patient were benign in nature, although the lesions were extraordinarily extensive, and excluded the possibility of neonatal malignant melanoma that had developed within a giant congenital naevus[11] or as skin metastases from the meninges or any other central nervous system compartment.

This case showed several interesting features. One was the pagetoid arrays of naevus cells that were found in the junctional zone. These are commonly associated with rapid spreading of lesions of pigmented naevi in a newborn, although these intraepidermal components sometimes resemble superficial spreading melanoma. The other features were myxoid changes in the dermis in the present case, probably indicating neural differentiation. These observations are consistent with those of Bastian *et al.*,[12] who previously described histological patterns of secondary proliferation in a congenital naevus during the neonatal period. These unique features might also be of use to differentiate proliferative nodules in giant congenital naevi from malignant melanoma, especially from neonatal malignant melanoma that develops within a giant congenital naevus,[11] which is notoriously difficult to diagnose.

In conclusion, the extensive neonatal proliferative nodules described in this report provide several characteristic histological patterns that can assist the diagnosis of pigmented nodular lesions in a giant congenital naevus and, consequently, reduce the risk of misdiagnosing these lesions as malignant melanoma, even in cases of extensive proliferative nodules such as this case.

References

1. Elder DE, Murphy GF. Melanocytic tumour of the skin. Benign melanocytic tumours (naevi). *Atlas of Tumour Pathology*, 3rd series. Washington DC: AFIP, 1991; 70–7.
2. Clark WH Jr, Elder DE, Guerry D. The pathogenesis and pathology of dysplastic naevi and malignant melanoma. In: *Pathology of the Skin* (Farmer ER, Hood AF, eds). East Norwalk, Connecticut: Appleton and Lange, 1990; 730–1.
3. Borbujo J, Jara M, Cortes L *et al.* A newborn with nodular ulcerated lesion on a giant congenital nevus. *Pediatr Dermatol* 2000; **17**: 299–301.
4. Lowes MA, Norris D, Whitfeld M. Benign melanocytic proliferative nodule within a congenital naevus. *Australas J Dermatol* 2000; **41**: 109–11.
5. Leech SN, Bell H, Leonard N *et al.* Neonatal giant congenital nevi with proliferative nodules. *Arch Dermatol* 2004; **140**: 83–8.
6. de Vooght A, Vanwijck R, Gosseye S *et al.* Pseudo-tumoral proliferative nodule in a giant congenital naevus. *Br J Plast Surg* 2003; **56**: 164–7.
7. McGowan JW, Smith MK, Ryan M, Hood AF. Proliferative nodules with balloon-cell change in a large congenital melanocytic nevus. *J Cutan Pathol* 2006; **33**: 253–5.
8. Herron MD, Vanderhooft SL, Smock K *et al.* Proliferative nodules in congenital melanocytic nevi: a clinicopathologic and immunohistochemical analysis. *Am J Surg Pathol* 2004; **28**: 1017–25.
9. Elder D, Elenitsas R. Benign pigmented lesions and malignant melanoma. In: Elder D, Elenitsas R, Jaworsky C, Johnson B, eds. *Lever's Histopathology of the Skin*, 8th edn. Philadelphia: Lippincott-Raven, 1997.
10. Giam YC, Williams ML, LeBoit PE *et al.* Neonatal erosions and ulcerations in giant congenital melanocytic nevi. *Pediatr Dermatol* 1999; **16**: 354–8.
11. Asai J, Takenaka H, Ikeda S *et al.* Congenital malignant melanoma: a case report. *Br J Dermatol* 2004; **151**: 693–7.
12. Bastian BC, Xiong J, Frieden IJ *et al.* Genetic changes in neoplasms arising in congenital melanocytic nevi. *Am J Pathol* 2002; **161**: 1163–9.

doi:10.1111/j.1600-0609.2007.00897.x European Journal of Haematology ISSN 0902-4441

CLINICAL PICTURE

Non-Hodgkin lymphoma preceded by recalcitrant eczema

A 34-yr-old woman visited us with 3-yr history of severe eczema over her whole body because of exacerbation of her skin symptoms. She was admitted to our hospital for detailed examination and treatment. On physical examination, up to 5-mm-sized, bright brown-coloured, excoriated papules and edematous blackish erythema were densely scattered over her whole body (Fig. 1A). Skin lesions were refractory to standard topical corticosteroid therapy. She developed a constellation of symptoms including remittent fever, malaise and a significant weight loss by as much as 10 kg for a month. We performed imaging studies to investigate underlying diseases because of an unusual course of skin lesions. Thoracic and abdominal CT scan disclosed multiple enlarged lymph nodes (Fig. 1B). Specimens from her right inguinal lymph node showed a marked, atypical infiltration of large CD20-positive cells, without any demonstrable follicular architecture. Southern blot analysis of immunoglobulin heavy-chain gene rearrangement proved the monoclonal nature of the infiltrated B cells. The diagnosis of diffuse large B-cell lymphoma was made. The patient received six cycles of rituximab, cyclophosphamide, adriamycin, vincristine and prednisone (R-CHOP) chemotherapy. After the R-CHOP cycles, she underwent high-dose chemotherapy and autologous peripheral blood stem cell transplantation. Pretransplant conditioning employed MCVC (ranimustine, carboplatin, etoposide and cyclophosphamide). She obtained partial lymphoma remission (Fig. 1D). Skin lesions completely regressed together with the lymphoma remission, and she has not since relapsed (Fig. 1C).

Pruritus is occasionally observed in patients with non-Hodgkin lymphoma. Recalcitrant eczema may represent as the itch–scratch cycle caused by severe itching due to lymphoma, although it is quite rare that intractable eczema leads to detection of underlying lymphoma. The pathomechanisms that lead to pruritus in patients with lymphoma are unclear. However, such a simple skin lesion is able to alert clinicians to an underlying malignancy, if the lesion is unusually chronic and difficult to manage.

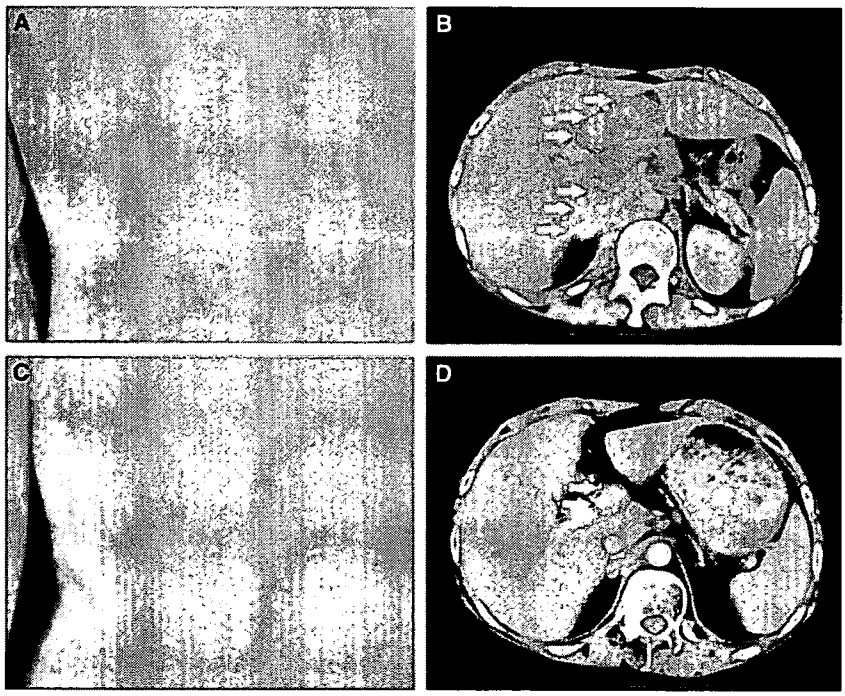

Figure 1 (A) Intractable eczema lead to the detection of (B) underlying diffuse large B-cell lymphoma. (C) Eczematous lesions disappeared together with (D) the lymphoma remission.

Ken Natsuga[1], Riichiro Abe[1], Hideyuki Ujiie[1], Akihiko Shibaki[1], Daisuke Sawamura[1], Mitsufumi Nishio[2], Katsuya Fujimoto[2], Takao Koike[2], Hiroshi Shimizu[1]
Department of [1]Dermatology and [2]Medicine II, Hokkaido University Graduate School of Medicine, Sapporo, Japan

Correspondence Ken Natsuga, MD, Department of Dermatology, Hokkaido University Graduate School of Medicine, North 15, West 7, Kita-ku, Sapporo 060-8638, Japan.
Tel: +81 11 716 1161 ext. 5962;
Fax: +81 11 706 7820;
e-mail: natsuga@med.hokudai.ac.jp

11 Anbar S, Westerhof W, Badawy N *et al.* The role of H1 and H2 receptor antagonists in inhibition of UVB-induced melanogenesis in guinea pigs. *15th Congress of the European Academy of Dermatology and Venereology*, 2006; Abstract FC16.4.

Conflicts of interest: none declared.

Neonatal vesiculopustular eruption of the face: a sign of trisomy 21-associated transient myeloproliferative disorder

DOI: 10.1111/j.1365-2133.2007.07877.x

SIR, Neonatal vesiculopustular eruptions suggest a number of differential diagnoses including both infectious and noninfectious aetiologies. We describe a phenotypically normal neonate with a vesiculopustular eruption arising from birth as the result of a transient myeloproliferative disorder (TMD) associated with mosaic trisomy 21.

In November 2005, a Japanese girl was born at 39 weeks' gestation, the second child of a healthy 25-year-old woman. Shortly after birth, bizarre vesiculopustular skin lesions were observed on her face, and rapidly increased in number with a tendency to appear at sites where pressure or dressings had been applied. There was no maternal history of genital herpes simplex virus infection, and application of topical aciclovir by the attending paediatrician failed to improve the skin lesions. She was referred to the dermatology clinic on day of life (DOL) 14.

Physical examination revealed 3- to 6-mm, reddish, small vesicular papules with yellowish crusts scattered on her face, especially on the cheeks (Fig. 1). Bacterial culture from the eruption resulted in a marginal growth of *Staphylococcus aureus*, *Enterococcus faecalis* and methicillin-resistant *S. aureus*. Skin biopsy of a papule on her left cheek revealed prominent infiltration of mononuclear cells with slightly atypical nuclei within the epidermis and upper dermis. There were no viral inclusions, ballooning or reticular degeneration in the epidermis (Fig. 2a). The myeloid lineage of these mononuclear cells was confirmed using myeloperoxidase staining (Fig. 2b).

Fig 1. Vesiculopustular eruption on the face of a phenotypically normal female neonate with transient myeloproliferative disorder.

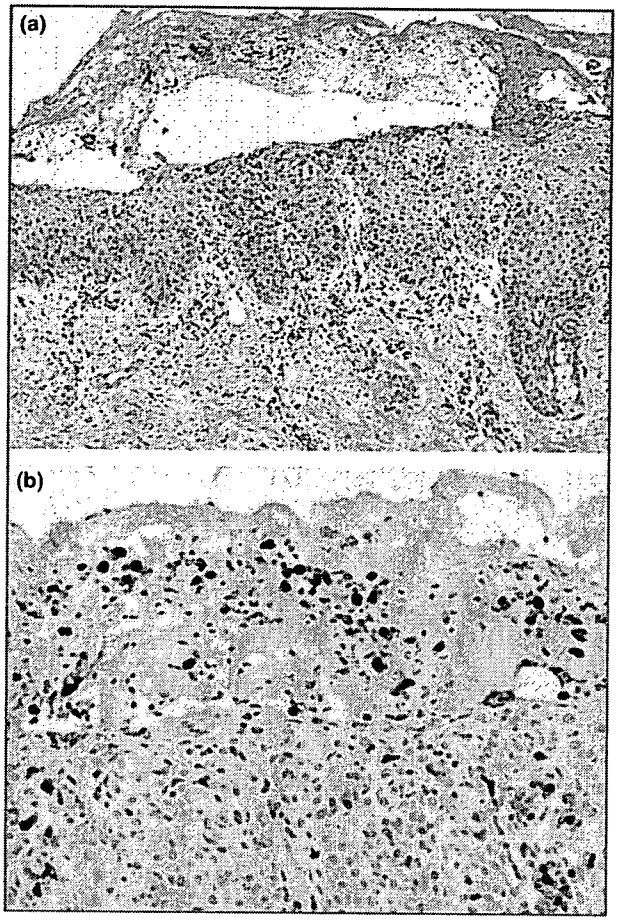

Fig 2. (a) Prominent infiltration of immature lymphoid cells with slightly atypical nuclei in the upper dermis and epidermis in a skin biopsy taken from the left cheek (haematoxylin and eosin; original magnification × 200). (b) Infiltrated cells were myeloid lineage or immature myeloid (myeloperoxidase staining; original magnification × 400).

The baby had experienced shortness of breath on DOL 4. At the time of this episode, the white blood cell (WBC) count was $99{\cdot}7 \times 10^9\ L^{-1}$, with blast cells. Acute myelogenous leukaemia (AML) was suspected; however, bone marrow aspiration demonstrated no blast cells. Thus she was diagnosed as having TMD. As TMD is known to occur mainly in infants with Down syndrome, peripheral blood fluorescence *in situ* hybridization (FISH) was performed. Although she was phenotypically normal, FISH analysis revealed mosaicism for trisomy 21. The vesiculopustular eruption was resistant to topical antibiotics (gentamicin or fusidic acid) and remained unchanged until DOL 17. Later, the eruption showed a tendency to improve as the WBC count decreased smoothly, and spontaneously cleared without any additional intervention at 2 months of age. Further follow-up of her blood counts at intervals of 3 months revealed no sign of haematological malignancy, and she remains healthy at 1 year of age.

Neonates with trisomy 21 have an increased risk of haematological abnormalities, including leukaemoid reaction, TMD and congenital leukaemia. TMD is a syndrome of spontaneously resolving hyperleucocytosis in infants, and is found almost exclusively in neonates with Down syndrome.[1] However, this disorder has also been reported in phenotypically normal neonates with trisomy 21 mosaicism.[2] Although TMD is known to follow a benign clinical course, some patients have developed secondary life-threatening haematological disorders after the improvement of TMD. Therefore, recent publications strongly recommend that patients with a history of TMD should undergo full blood counts at intervals of 3–6 months during the first years of life.[3] The most frequent disease which occurs subsequently to TMD is AML, usually megakaryoblastic type (AML-M7), and the rate of incidence is relatively high. Zipursky *et al.*[4] reported that about 25% of infants who recovered from TMD developed AML-M7. Genetic research is in progress, and a recent study has revealed that almost all cases of TMD were associated with somatic *GATA1* mutations,[3] found initially in AML-M7 in patients with Down syndrome.[5,6] In addition, Hasle *et al.*[7] suggested that persistently upregulated Wilms tumor 1 gene expression level might be associated with an elevated risk of subsequent development of AML.

At the initial visit, we diagnosed this case as neonatal pustular disease, and several differential diagnoses were considered. Infantile acne is a well-known disorder in which a pustular eruption forms on the face of neonates. However, in general, this disorder does not occur immediately after birth, and the lesions usually comprise tiny pustules with comedones. Histological findings ruled out erythema neonatorum, eosinophilic pustular folliculitis of infancy and incontinentia pigmenti, because there was no eosinophil infiltration. The infant had no vesiculopustular eruption at the time of birth, and no postlesional pigmentation was observed during her clinical course, and thus transient neonatal pustulosis was excluded. Neonatal listeriosis, caused by *Listeria monocytogenes*, can manifest pustular eruptions; however, this condition was ruled out because the amniotic fluid was not stained at her birth, no systemic symptoms suggesting sepsis or meningitis were observed, and bacterial culture failed to identify L. *monocytogenes*.

Thirteen cases of vesiculopustular eruption have previously been reported in patients with TMD associated with trisomy 21.[8–12] These cases share similar clinical features. The skin lesions appeared mainly on the face either from birth or soon after birth, especially where pressure was applied. Most of these cases with skin eruptions followed a benign clinical course, and the skin lesions spontaneously disappeared over weeks to years as the WBC count normalized. However, two fatal cases are reported among these 13 cases including a case with secondary development of AML.[9]

In conclusion, clinicians should consider the possibility of TMD associated with trisomy 21 mosaicism, when they encounter an unknown vesiculopustular eruption in phenotypically normal neonates. Careful follow up is recommended in such cases because of the possibility of secondary haematological malignancy.

Departments of Dermatology and
*Paediatrics, Hokkaido University
Graduate School of Medicine,
N15 W7, Kita-ku, Sapporo 060-8638, Japan
Correspondence: Akihiko Shibaki.
E-mail: ashibaki@med.hokudai.ac.jp

R. Moriuchi
A. Shibaki
K. Yasukawa
T. Onozuka
T. Sato*
M. Kaneda*
A. Iguchi*
R. Kobayashi*
H. Shimizu

References

1 Engel R, Hammond D. Transient congenital leukemia in 7 infants with mongolism. *J Pediatr* 1964; **65**:303–5.
2 Heaton DC, Fitzgerald PH, Fraser J, Abbott GD. Transient leukemoid proliferation of the cytogenetically unbalanced +21 cell line of a constitutional mosaic boy. *Blood* 1981; **57**:883–7.
3 Dixon N, Kishnani PS, Zimmerman S. Clinical manifestations of hematologic and oncologic disorders in patients with Down syndrome. *Am J Med Genet C Semin Med Genet* 2006; **142**:149–57.
4 Zipursky A, Brown EJ, Christensen H *et al.* Leukaemia and/or myeloproliferative syndrome in neonates with Down's syndrome. *Semin Perinat* 1997; **21**:97–101.
5 Wechsler J, Greene M, McDevitt MA *et al.* Acquired mutations in *GATA1* in the megakaryoblastic leukemia of Down syndrome. *Nat Genet* 2002; **32**:148–52.
6 Mundschau G, Gurbuxani S, Gamis AS *et al.* Mutagenesis of *GATA1* is an initiating event in Down syndrome leukemogenesis. *Blood* 2003; **101**:4298–300.
7 Hasle H, Lund B, Nyvold CG *et al.* *WT1* gene expression in children with Down syndrome and transient myeloproliferative disorder. *Leuk Res* 2006; **30**:543–6.
8 Nijhawan A, Baselga E, Gonzalez-Ensenat MA *et al.* Vesiculopustular eruptions in Down syndrome neonates with myeloproliferative disorders. *Arch Dermatol* 2001; **137**:760–3.
9 Burch JM, Weston WL, Rogers M, Morelli JG. Cutaneous pustular leukemoid reactions in trisomy 21. *Pediatr Dermatol* 2003; **20**:232–7.
10 Solky BA, Yang FC, Xu X, Levins P. Transient myeloproliferative disorder causing a vesiculopustular eruption in a phenotypically normal neonate. *Pediatr Dermatol* 2004; **21**:551–4.
11 Viros A, Garcia-Patos V, Aparicio G *et al.* Sterile neonatal pustulosis associated with transient myeloproliferative disorder in twins. *Arch Dermatol* 2005; **141**:1053–4.
12 Wirges ML, Stetson CL, Oliver JW. Pustular leukemoid reaction in a neonate with Down syndrome. *J Am Acad Dermatol* 2006; **54**:S62–4.

Conflicts of interest: none declared.

Planar xanthoma due to cholestasis in graft versus host disease

DOI: 10.1111/j.1365-2133.2007.07878.x

Sir, Bone marrow transplantation is increasingly being used to treat a wide variety of malignant and nonmalignant diseases.[1,2] As the treatment of infections improves, graft-versus-host disease (GVHD) emerges as one of the most

doi: 10.1111/j.1365-2230.2006.02262.x

Giant dermatofibroma: a rare variant of dermatofibroma preferentially developing on the lower limbs

D. Hoshina, A. Shibaki, S. Aoyagi, K. Kimura and H. Shimizu

Department of Dermatology, Hokkaido University Graduate School of Medicine, N15 W7, Kita-ku, Sapporo 060–8638, Japan

A 20-year-old man presented to our outpatient clinic with a 3-year history of a slowly growing nodule on his right leg. Physical examination revealed a brown, firm nodule, 50 mm in diameter, which was immobile owing to the adhesion to the subcutaneous tissue (Fig. 1a). The surface of the nodule was moderately hyperkeratotic and partly covered with brown crusts. An initial incisional biopsy demonstrated an irregularly arranged dense proliferation of fibroblast-like cells throughout the dermis and superficial subcutaneous tissue. Magnetic resonance imaging demonstrated invasion close to the fascia of the anterior tibial muscle (Fig. 1b). A simple surgical excision was made for diagnosis and treatment.

Histopathological examination revealed a relatively sparse proliferation of fibroblast-like tumour cells without nuclear atypia throughout the entire dermis (Fig. 2a). The overlying epidermis demonstrated moderate hyperkeratosis (Fig. 2b). The tumour cells were loosely arranged within the mature collagen bundles (Fig. 2c) and partially extended into the superficial subcutaneous tissue along the fibrous septa (Fig. 2d). Immunohistochemical examination demonstrated a lack of CD34 expression in the proliferating tumour cells. From the histopathological and immunohistochemical features, a diagnosis of giant dermatofibroma (DF) was made.

DF is a benign cutaneous tumour, generally <20 mm in diameter.[1] However, these tumours sometimes enlarge and may be misdiagnosed as malignant tumours, such as dermatofibrosarcoma protuberans (DFSP). Giant DF is a clinical variant of DF, designated by Danckaert and Karassik in 1975[1] and characterized by its unusually large size. Although there is no clear definition of the size for the diagnosis of giant DF, Requena *et al.*[2] used a size larger than 35 mm for the diagnosis of giant DF in their study. In previous reports, the size of the tumour ranged from 35 to 120 mm, and almost all the lesions were located on the lower limbs.[1–3] No recurrence after surgical excision has been reported to date.[2]

Distinguishing giant DF from malignant fibrous tumours, especially DFSP, may be difficult, owing to its unusual clinical appearance. Although histopathological examination reveals conventional features of DF in most cases, an incisional biopsy specimen from the tumour may demonstrate architectural features similar to DFSP. In order to distinguish between the two entities of giant DF and DFSP, several reports have suggested that immunohistochemical analysis of CD34 and factor XIIIa expression is useful.[4] However, even these methods could fail to lead to a diagnosis because there may be staining variability among different cases. Focal CD34 reactivity may be demonstrated in some DF cases,[4,5] whereas some DFSPs uncharacteristically express factor XIIIa, but not CD34.[4,5] Recently, Cribier *et al.* reported that immunohistochemical staining of stromelysin 3 (ST3) may be useful for the distinction in such problematic cases. In their study, none of the 40 DFSP cases expressed ST3, while all 40 DF cases, including 10 giant DFs, expressed ST3.[5]

In our case, initial incisional biopsy was insufficient to permit a definite diagnosis to be made. Careful histopathological re-evaluation of the surgical specimens revealed that most of the tumour showed the typical histopathological features of DF. In addition, the negative result of immunohistochemical staining with anti-CD34 supported the diagnosis of giant DF.

We suggest that a thorough histopathological examination of large tissue samples from the tumour, together with immunohistochemical staining, is recommended for the correct diagnosis of giant DF.

Correspondence: Dr Akihiko Shibaki, MD, PhD, Department of Dermatology, Hokkaido University Graduate School of Medicine, North 15 West 7, Kita-ku, Sapporo 060-8638, Japan.
E-mail: ashibaki@med.hokudai.ac.jp

Conflict of interest: none declared.

Accepted for publication 30 June 2006

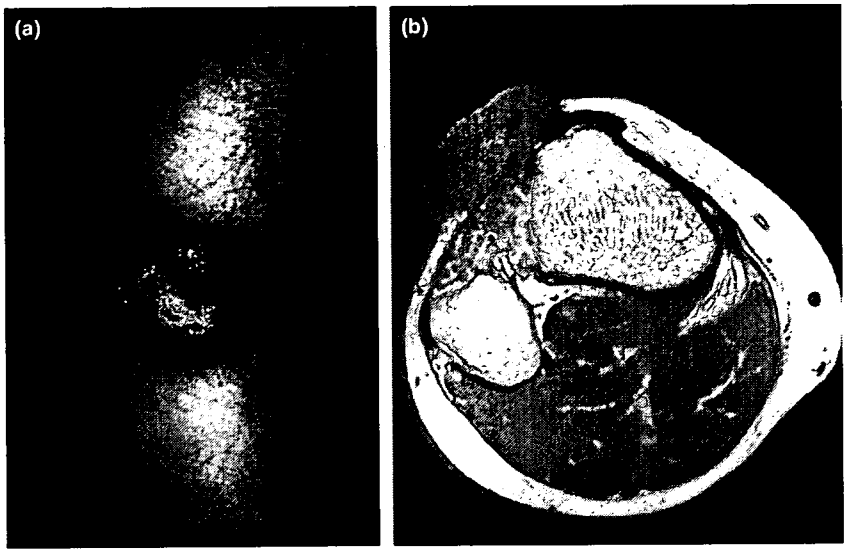

Figure 1 (a) Brown, firm nodule, 50 mm in diameter, immobile owing to adhesion to the subcutaneous tissue; (b) magnetic resonance imaging demonstrated invasion close to the fascia of the anterior tibial muscle.

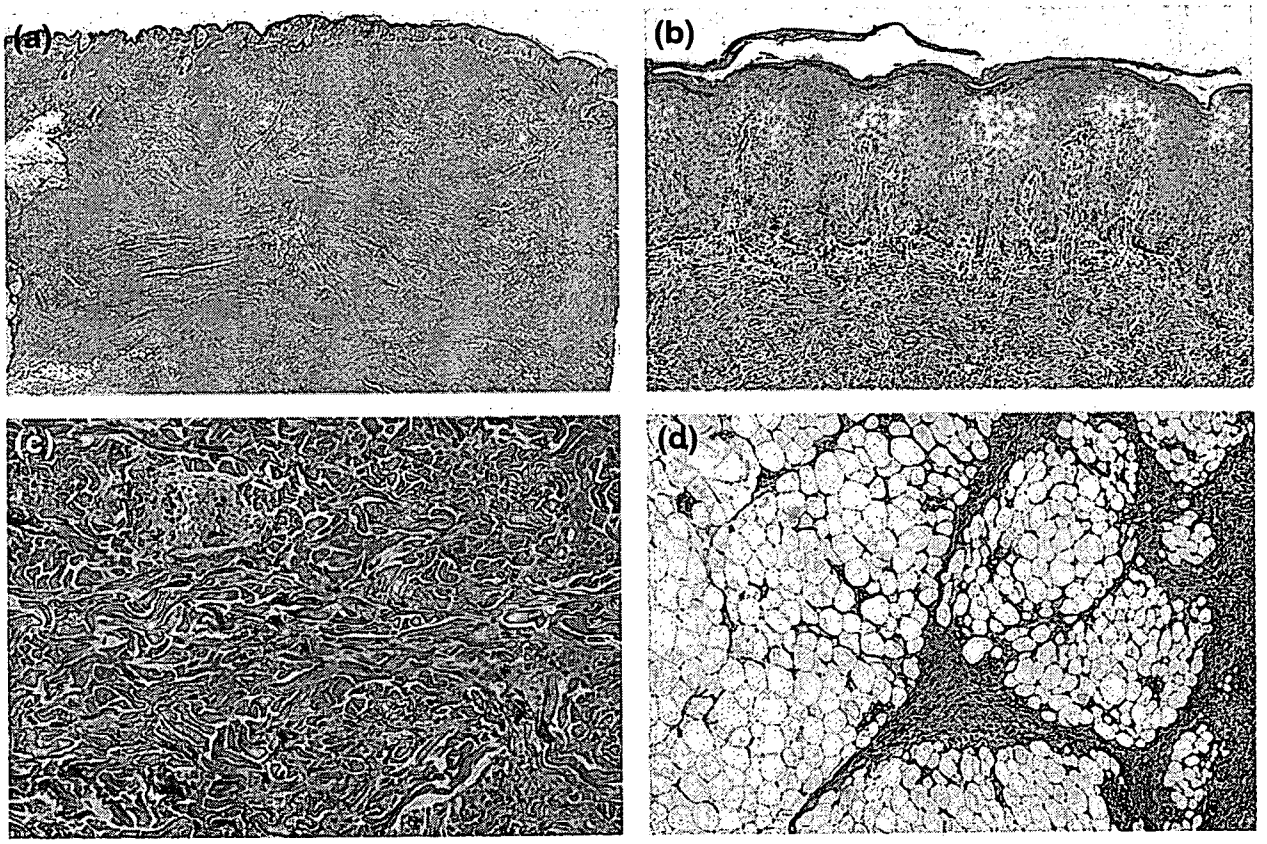

Figure 2 (a) A relatively sparse proliferation of fibroblasts without nuclear atypia, which produced mature collagen bundles throughout the entire tumour. (b) the overlying epidermis demonstrated moderate hyperplasia; (c) most of the tumour was occupied by an area with a sparse number of cells, comprised of plump spindle cells producing mature collagen bundles; (d) the subcutaneous invasion preserved the fat lobules. Haematoxylin and eosin, original magnification (a) ×5, (b–d) ×100.

References

1 Danckaert B, Karassik SL. Dermatofibroma: An usual presentation. *Cutis* 1975; **16**: 245–7.

2 Requena L, Farina MC, Fuente C *et al.* Giant dermatofibroma. A little known clinical variant of dermatofibroma. *J Am Acad Dermatol* 1994; **30**: 714–19.

3 Goolman HB, Sanders LJ, Porter MC. Benign fibrous histiocytoma of the foot: a literature review and case report. *Cutis* 1990; **46**: 223–6.

4 Goldblum JR, Tuthill RJ. CD34 and factor-XIIIa immunoreactivity in dermatofibrosarcoma protuberans and dermatofibroma. *Am J Dermatopathol* 1977; **19**: 147–53.

5 Cribier B, Noacco G, Peltre B, Grosshans E. Stromelysin 3 expression: a useful marker for the differential diagnosis dermatofibroma versus dermatofibrosarcoma protuberans. *J Am Acad Dermatol* 2002; **46**: 408–13.

Mesenchymal Stem Cells Are Recruited into Wounded Skin and Contribute to Wound Repair by Transdifferentiation into Multiple Skin Cell Type[1]

Mikako Sasaki,[2] Riichiro Abe,[2] Yasuyuki Fujita, Satomi Ando, Daisuke Inokuma, and Hiroshi Shimizu[3]

Mesenchymal stem cells (MSCs) can differentiate not only into mesenchymal lineage cells but also into various other cell lineages. As MSCs can easily be isolated from bone marrow, they can be used in various tissue engineering strategies. In this study, we assessed whether MSCs can differentiate into multiple skin cell types including keratinocytes and contribute to wound repair. First, we found keratin 14-positive cells, presumed to be keratinocytes that transdifferentiated from MSCs in vitro. Next, we assessed whether MSCs can transdifferentiate into multiple skin cell types in vivo. At sites of mouse wounds that had been i.v. injected with MSCs derived from GFP transgenic mice, we detected GFP-positive cells associated with specific markers for keratinocytes, endothelial cells, and pericytes. Because MSCs are predominantly located in bone marrow, we investigated the main MSC recruitment mechanism. MSCs expressed several chemokine receptors; especially CCR7, which is a receptor of SLC/CCL21, that enhanced MSC migration. Finally, MSC-injected mice underwent rapid wound repaired. Furthermore, intradermal injection of SLC/CCL21 increased the migration of MSCs, which resulted in an even greater acceleration of wound repair. Taken together, we have demonstrated that MSCs contribute to wound repair via processes involving MSCs differentiation various cell components of the skin. ***The Journal of Immunology,*** **2008, 180: 2581–2587.**

Bone marrow has an extremely complex cellular arrangement of bone marrow stroma, to maintain the hemopoietic microenvironment. Other than hemopoietic stem cells and differentiated lineages, bone marrow contains a subset of nonhemopoietic cells, mesenchymal stem cells (MSCs)[4] that account for roughly 0.01–0.001% of the bone marrow derived cell population (1). These rare, heterogeneous cells have the capacity to proliferate and differentiate into mesenchymal lineage cells such as osteoblasts, adipocytes, and chondrocytes (1, 2) (3, 4). Thus, MSCs are thought to be the key in maintaining the bone marrow microenvironment. Various mesenchymal tissues such as s.c. fat also contain MSCs (5).

Recent reports show that MSCs may have the ability to differentiate into other lineage cells in vitro, such as endothelial cells (6, 7), neural cells (8, 9) and hepatocytes (10, 11). In vivo studies have also shown that MSCs can differentiate into tissue-specific cells in response to cues provided by different organs (12).

In addition to pluripotency, MSCs are known to have immunosuppressive effects involving various mechanisms, resulting in evading the allogeneic host immunosurveillance system (13). Therefore, recent studies have suggested that MSCs are promising candidates for cell-based tissue engineering, to repair or replace important damaged tissues (14) such as after myocardial infarction (15), and spinal injury (16). However, there have been no investigations into whether the introduction of MSCs into skin wounds is effective or not.

So far, MSCs have already been used in several clinical trials including neurological diseases and spinal injury (17, 18), with results that have fallen short of any high expectations. It has been speculated that one of reasons was an insufficient knowledge of physiological behavior of MSCs. The detailed mechanisms of specific cell type differentiation from MSCs still remain to be identified. To better handle this potentially useful cell type and provide further promising novel regenerative cell therapies, we urgently require a much greater in-depth knowledge of MSCs to make better use of them in therapies.

We hypothesize that induction of mechanical stress in skin results in the release of various cytokines, especially chemokines which recruit blood-circulating MSCs (19). At the same time, these chemokines increase bone marrow stem cell mobility, thereby, facilitating MSCs mobilization into the peripheral blood and into sites of wound healing. Accumulating MSCs at wounded sites are able to transdifferentiate into multiple skin component cell types, thus contributing to wound repair.

In this study, we cultured MSCs in various culture medium, and have identified certain conditions under which MSCs efficiently differentiate into keratinocytes in vitro. Additionally, we have i.v. injected MSCs into wounded mice, and have investigated whether

Department of Dermatology, Hokkaido University Graduate School of Medicine, Sapporo, Japan

Received for publication July 25, 2007. Accepted for publication December 1, 2007.

The costs of publication of this article were defrayed in part by the payment of page charges. This article must therefore be hereby marked *advertisement* in accordance with 18 U.S.C. Section 1734 solely to indicate this fact.

[1] This work was supported in part by grants-in-aid for Scientific Research (no. 13357008 to H.S. and no. 15790563 to R.A.) and the Project for Realization of Regenerative Medicine from the Ministry of Education, Science, Sports and Culture of Japan (to H.S.), and Health and Labor Sciences Research grants from the Ministry of Health, Labor and Welfare of Japan (no. H13-Measures for Intractable Disease-02 and H16-Measures for Intractable Disease-02 to H.S.).

[2] M.S and R.A. contributed equally to this work.

[3] Address correspondence and reprint requests to Dr. Hiroshi Shimizu, Department of Dermatology, Hokkaido University Graduate School of Medicine, N 15 W 7, Kita-ku, Sapporo 060-8638, Japan. E-mail address: shimizu@med.hokudai.ac.jp

[4] Abbreviations used in this paper: MSC, mesenchymal stem cell; FISH, fluorescence in situ hybridization; SMA, smooth muscle actin; TARC, thymus and activation regulated chemokine; MIP, macrophage inflammatory protein; SLC, secondary lymphoid tissue chemokine; CTACK, cutaneous T cell-attracting chemokine; HPF, high power field.

MSCs migrate and become engrafted into wounded skin to promote wound healing.

Materials and Methods

Isolation and culture of MSCs from mouse bone marrow

Bone marrow-derived cells were collected by flushing the femurs and tibias from C57BL/6 and GFP-transgenic (under control of β-actin promoter) male mice (The Jackson Laboratory). These cells were cultured in MesenCult basal medium containing MSC stimulatory supplements (StemCell Technologies). After 48 h, the nonadherent cells were removed and fresh medium was added to the cells. Medium was changed every 2 or 3 days. The adherent spindle-shaped cells were further propagated for three passages.

Flow cytometry

Cultured MSCs were analyzed by flow cytometry (FACS Calibur; BD Biosciences). Cells were incubated with anti-CD31, CD34, CD44, CD90 (BD Biosciences), CD29 (Cymbus Biotechnology), and cytokeratin 14 (Chemicon) and secondary FITC-conjugated Abs (The Jackson Laboratory).

Differentiation culture of MSCs for mesenchymal lineage

MSCs were placed in basic medium, consisting DMEM (Invitrogen Life Technologies), 10% FBS, 1% penicillin, 1% streptomycin, 1% amphotericin B, and then specific supplements for mesenchymal lineage differentiation were added (20). Adipogenic differentiation was induced by basic medium with 0.5 μM dexamethazone, 0.5 mM 3-isobutyl-1-methylxanthine, and 0.1 mM indomethacine (Sigma-Aldrich) (21). Osteogenic differentiation was achieved by basic medium containing 0.1 μM dexamethazone, 50 μM ascorbic acid, and 10 mM β-glycerophosphate (Sigma-Aldrich) (22). Chondorogenic differentiation was induced by basic medium containing 50 μM ascorbic acid, 0.1 μM dexamethazone, 10 ng/ml TGF-β (R&D Systems), 40 μg/ml L-proline (Sigma-Aldrich), and 100 μg/ml sodium pyruvate (Wako) (23). Each specific differentiation medium was changed every 2–3 days. Confirmation of differentiation of the cells to adipocytes, osteocytes and chondrocytes were performed by staining with oil red O, Von Kossa, and toluidine blue, respectively.

Induction of MSC into keratinocyte differentiation

MSCs were plated into 8-well slide glass chamber and cultured in keratinocyte basal medium (Invitrogen Life Technologies) containing 0.5 nM bone morphogenetic protein-4 (BMP-4) (R&D Systems), 0.3 mM ascorbic acid, 0.5 μg/ml hydrocortisone or 3 ng/ml human epithelium growth factor (Cambrex). After 7 days culture, MSCs were stained with cytokeratin 14 Abs (Chemicon).

Intravenous injection of MSCs into the wounded mice

All animal procedures were conducted according to guidelines provided by the Hokkaido University Institutional Animal Care and Use Committee under an approved protocol. Female C57BL/6 mice were anesthetized and 10-mm full thickness punch biopsy wounds were made. One million MSCs derived from male GFP transgenic mice were injected into the tail vein of back skin-injured mice. All wounds were repaired within 2 wk. When the wound was repaired, the area skin was collected and analyzed. Furthermore, wound area was measured in mice with and without MSC injection.

To calculate migrated MSCs in wound skin, wound sites were removed 3 days later and examined for the presence of GFP^+ MSCs by quantitative flow cytometric analysis following proteolytic digestion. For quantitative flow cytometric analysis, excised skin (250 mg biopsy/animal) was chopped into small fragments, then incubated for 1 h at 37°C in RPMI 1640 containing 10% FBS, 2 mg/ml collagenase, and 20 mg/ml DNase I. The resulting single-cell suspension was examined by flow cytometry to determine the number of fluorescent fibrocytes present.

Fibroblasts (1×10^6) cultured from adult GFP transgenic mouse skin were injected into the tail vein of back skin-injured mice. After 8 days, wound sites were removed to analyze.

Immunofluorescence staining

Skin sections were stained with anti-GFP Ab (Molecular Probes). In addition, skin sections were treated with primary Abs against CD45, CD31, pan-cytokeratin (Progen), α-smooth muscle actin (SMA; LAB VISION), and CCR7 (Santa Cruz Biotechnology). Secondary Abs conjugated to rhodamine-isothiocyanate (Southern Biotechnology) were used for fluorescence staining detection together with a confocal laser scanning fluorescence microscope (FV1000; Olympus).

Detection of X- and Y-chromosomes by fluorescence in situ hybridization (FISH) analysis

To investigate whether the GFP positive cells in the skin of MSC injected mice were the result of transdifferentiation or cell fusion with host cells, we used MSCs of a different sex from the recipient mice, and investigated the tissue using FISH analysis. X- and Y-chromosomes were detected using the Dual Color Detection kit (Cambio) according to the manufacturer's protocol (Cy5 for Y chromosomes and Cy3 for X chromosomes) and immediately viewed with a confocal laser scanning fluorescence microscope.

Chemokine receptor expression in MSCs

Total RNA was isolated from MSCs. RT-PCR analysis of mRNA from chemokine receptors and GAPDH were performed in a thermocycler (GeneAmp PCR system 9600; PerkinElmer). Primers are as follows: CXCR4 (sense: 5′-ACTGCATCATCATCTCCAAGC-3′, antisense: 5′-CTCTCGAAGTCACATCCTTGC-3′); CCR4 (sense: 5′-TCTACAGCGGCATCTTCTTCAT-3′, antisense: 5′-CAGTACGTGTGGTTGTGCTCT-3′); CCR5 (sense: 5′-CTGGCCATCTCTGACCTGTTTTTC-3′, antisense: 5′-CAGCCCTGTGCCTCTTCTTCTCAT-3′); CCR7 (sense: 5′-ACAGCGGCCTCCAGAAGAAGAGCGC-3′, antisense: 5′-TGACGTCATAGGCAATGTTGAGCTG-3′); CCR10 (sense: 5′-GGCCCTGACTTTGCCTTTTG-3′, antisense: 5′-GCTGCCAGTAGATCGGCTGT-3′); GAPDH (sense: 5′-GAGGGGCCATCCACAGTCTTC-3′, antisense: 5′-CATCACCATCTTCCAGGAGCG-3′).

MSCs were incubated with anti- CXCR4, CCR4, CCR5 (BD Pharmingen), CCR7 (Santa Cruz Biotechnology), and CCR10 (Calbiochem) and then analyzed by flow cytometry as described above.

Chemotaxis assay

MSCs migration was evaluated using a Chemotaxicell (Kurabo) according to the manufacturer's instructions. The contents of the upper and lower chambers were separated by polycarbonate filter (8-μm pore size). MSCs were resuspended at 1.0×10^5/100 μl in Mesencult basal medium and seeded in the upper chamber. Recombinant monokine induced by IFN-γ, stromal derived factor 1, thymus and activation regulated chemokine (TARC), macrophage inflammatory protein (MIP)-3α, secondary lymphoid tissue chemokine (SLC/CCL21) and cutaneous T cell-attracting chemokine (CTACK) (R&D Systems) were used as chemoattractants in the lower chamber. The chambers were incubated overnight at 37°C. Results are expressed as number of migrated cells in lower chamber. To confirm CCR7 expression, migrated MSC in SLC/CCL21 chemotaxis assay were stained with CCR7 Ab (Santa Cruz Biotechnology).

Wound healing analysis

Female C57BL/6 mice were anesthetized and 10 mm full-thickness punch biopsy wounds were made. One million MSCs derived from male GFP transgenic mice were injected into the tail vein immediately after injury. Subsequently, the chemokine (SLC/CCL21, TARC, or CTACK; a total of 3 μg in 100 μl) or PBS (100 μl), as vehicle-only control, was intradermally injected into the periphery of the wounds. Standardized images of wounds were recorded using a digital camera for analysis of daily wound sizes.

Induction of MSC into endothelial cell differentiation

MSCs were plated into fibronectin coated 8-well slide glass chamber and cultured in DMEM containing with 50 ng/ml VEGF, 10 ng/ml bFGF, 3% FBS and 0, 1, 10, or 100 ng/ml SLC/CCL21. After 7 days culture, MSCs into endothelial cell differentiation were evaluated by CD31 Immunofluorescence staining.

Results

Characterization of isolated MSCs

Cell surface markers were assessed using flow cytometry to characterize isolated MSCs. MSCs expressed CD29, CD44,and CD90, but not CD34 and CD31 (Fig. 1*A*) consistent with previous reports (22, 24). MSCs were further characterized by confirming their ability to undergo specific adipogenic, osteogenic, and chondrogenic differentiation. These cells were positive for oil red O staining, Von Kossa's staining, and toluidine blue staining, indicating adipogenic, osteogenic, and chondrogenic respective cell type differentiation (Fig. 1, *B–D*). Only cells that met these criteria were used in subsequent experiments.

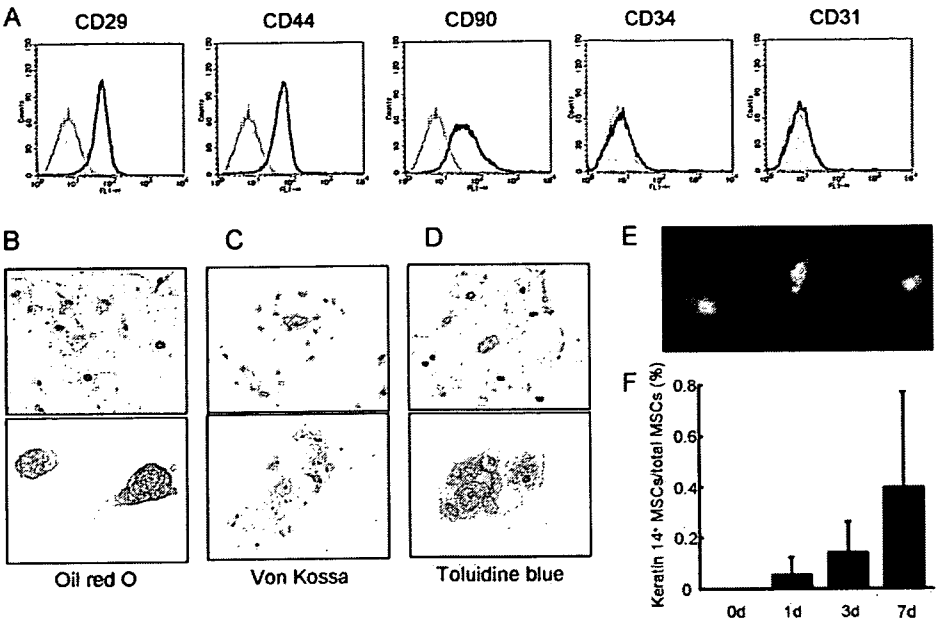

FIGURE 1. MSCs have a potential to differentiate into keratinocyte. *A*, Cell surface markers of MSCs were assessed using FACS. MSCs expressed CD29, CD44, and CD90, but not CD34, CD31. *B*, Adipogenic differentiation was revealed with oil red O staining. *C*, Osteogenic differentiation was confirmed by Von Kossa's staining. *D*, The chondorogenic potential of MSCs was determined by staining for toluidine blue. In *B–D, upper panels* are before differentiation induction, and *lower panels* are after differentiation induction, representatively. To investigate whether MSCs differentiate into keratinocytes, we cultured MSCs in various condition medium. *E*, MSCs cultured for 7 days were stained with cytokeratin 14 (green). Red fluorescence is nuclear staining by propidium iodide. *F*, The percentage of keratin 14 + MSCs in total MSCs at 0, 1, 3, and 7 day keratinocyte differentiation culture.

Cultured MSCs express keratin14

Recent reports have shown that MSCs can differentiate into various cell types. In skin cells, endothelial cells, pericytes, monocytes/macrophage, and adipocytes have been reported (24, 25). However, it is currently unknown whether MSCs can differentiate into keratinocytes. For that reason, we assessed whether MSCs can differentiate into keratinocytes in vitro. MSCs were exposed to 0.5 nM BMP-4 at different days of culture. Keratin 14 positive cells were presumed to identify MSC transdifferentiated keratinocytes. There were no keratin 14-positive cells at the beginning of culture, as bone marrow cells. Enhancement of keratinocyte commitment (0.48%) was clearly observed when 0.5 nM BMP-4 was added for 7 days (Fig. 1*F*).

MSCs differentiate into multiple skin cell types

Recent reports (22) have shown that MSCs were mobilized and differentiate into cardiomyocytes after myocardial infarction. Furthermore transplanted MSCs improved cardiac function in dilated cardiomyopathy (26). For that reason, we speculated that MSCs may differentiate into multiple skin cell types during wound healing. GFP transgenic mouse-derived MSCs were injected i.v. into injured mice. When wound repaired, the area skin was collected and performed immunofluorescence staining. GFP positive cells were colocalized with pan-cytokeratin (Fig. 2, *Aa–c*), CD31 (endothelial cell marker, Fig. 2, *Ad–f*), and α-SMA (myofibroblast and pericyte marker; Fig. 2, *Ag–i*). The number of GFP-positive, pan-cytokeratin-positive cells is1.0/high power field (HPF), and the percentage of GFP-positive in all pan-cytokeratin-positive cells is 0.14% (Table I). The number of MSCs that differentiated into endothelial cells was 4.7/HPF, and 13.2% of endothelial cells were GFP positive. In particular, 33.0% of pericytes (recognized as α-SMA-positive, CD31-negative and located close to the capillary (27)) were differentiated from injected MSCs. Although GFP-positive macrophages were also detected (1.5/HPF and 2.4%), no GFP-positive adipocytes were found. In addition, very few GFP-positive monocytes/macrophages (CD11b positive) were also found (data not shown).

To exclude the possibility that skin cell differentiation was the result of spontaneous cell fusion, we analyzed the presence of X and Y chromosomes using FISH methods. If MSCs and recipient skin cells were fused, these cells would contain XXXY chromosomes. Although we analyzed in total $\sim 1 \times 10^4$ cells, we detected no GFP-positive cells containing XXXY chromosomes. All GFP positive cells contain XY chromosomes (Fig. 2*B*) indicating that the incidence of MSCs and skin cell fusion is an extremely rare event.

MSCs migrate in response to specific chemokine gradients

Several papers have reported (28, 29) that MSCs constitutively express various chemokine receptors such as CCR1, CCR7, CCR9, CXCR4, CXCR5, and CXCR6. If chemokine/chemokine receptor interactions contribute to the recruitment of MSCs to damaged tissues, a specific chemokine should be up-regulated in the target tissue together with a partner receptor expressed on the MSCs. The ability of MSCs to migrate in response to chemotactic signals was investigated using a chemotaxis assay.

Chemokine receptor expression on MSCs were examined to determine potential migratory reaction to stimuli. MSCs expressed

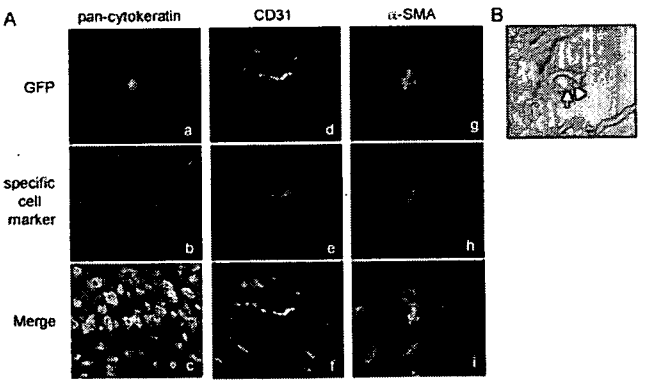

FIGURE 2. MSCs transdifferentiate into multiple skin cell type in wound site. *A*, MSC differentiate into multiple components of the skin. GFP positive cells (green) were colocalized with (*a–c*) pan-cytokeratin (red), (*d–f*) CD31(red), and (*g–i*) α-SMA (red). Nuclear staining (*c* and *f*) and CD31 (i) are blue. These data suggests MSCs were differentiated into keratinocytes, endothelial cells, and pericytes, respectively. *B*, Detection of X and Y chromosomes using FISH methods. All GFP positive cells contains XY chromosomes. Arrow (blue), Y; arrow head (red), X.

Table I. *MSC differentiated into various cell component of the skin*

	Number of Differentiated MSCs/HPF (×40)	MSC-Derived, Specific Cell Marker$^+$ Cell (%) (Number of GFP$^+$, Cell Marker$^+$/Number of Cell Marker$^+$)
Keratinocyte	1.0	0.14 (4/2828)
Endothelial cell	4.7	13.2 (24/182)
Macrophage	1.5	2.4 (3/129)
Pericyte	0.2	33.0 (5/15)

the transcripts for CCR4, CCR5, CCR7, and CCR10. Transcripts for other chemokine receptors were not detected. Protein expression was determined by flow cytometry analysis. CCR4, CCR5, CCR7, CCR10, and CXCR4 were also expressed in 14.3, 19.9, 10.0, and 38.0% of MSCs, respectively (Fig. 3*A*). These data are consistent with previous report that showed a minority of MSCs (2–25%) were expressed as a restricted set of chemokine receptors (29, 30).

To confirm that these receptors were actually functional in these cells, in vitro chemotaxis assays were undertaken. The following ligand-receptor combinations were investigated: TARC for CCR4, MIP-3α for CCR5, SLC/CCL21 for CCR7, and CTACK for CCR10. Neither CTACK nor MIP-3α enhanced MSC migration. In contrast, SLC/CCL21 and TARC induced MSCs' migration in a dose-dependent manner (Fig. 3*B*). Indeed, migrated MSCs induced by SLC/CCL21 in chemotaxis assay were almost all positive of CCR7 expression (Fig. 3*C*). Furthermore, in wound site of MSC injected mice, injected MSCs (GFP positive) expressed CCR7 (Fig. 3*D*).

SLC/CCL21 specifically led to the accumulation of MSCs in wounded skin and accelerated MSCs-induced wound healing

We analyzed the number of injected MSC (1×10^6) which accumulated in the skin wound. Using flow cytometry, 7.4×10^2 MSC were detected in the wound skin at 3 day after wound, and tend to decrease (Fig. 4*A*). To assess the ability of MSC recruitment by these chemokines in vivo, we intradermally injected these chemokines to the periphery of wounded skin in MSCs injected mice. The number of GFP-positive cells in the wound sites was then calculated, when the wound was repaired (each group, $n = 5$). Although TARC failed to influence the number of MSCs compared with controls, SLC/CCL21 significantly increased the number of GFP-positive MSCs in wounded skin (Fig. 4*B*). Time course analysis of the number of MSCs (2, 6, and 12 wk) showed the number of MSCs were gradually decreased (Fig. 4*C*). The quality of the wound was not significant difference between healed skin of MSC injected mice and that of control mice zt 15 days (Fig. 4*D*). In addition, the number of GFP$^+$ endothelial cells showed a trend to increase, and the number of GFP$^+$ pericytes increased significantly compared with control (Fig. 4*E*). We therefore surmised that SLC/CCL21 was capable of attracting MSCs, which participated in the host skin angiogenic wound response.

Furthermore, to evaluate the contribution of MSCs in reducing the wound area at 8 days, we measured wound size. Quantification of wound size demonstrated only 9.3 mm^2 in MSCs injected-mice, compared with 23 mm^2 in control mice (Fig. 4*F*). Wound size in the mice with fibroblasts injection was not significantly different from those of control mice (data not shown). MSCs injected-mice repaired wounds faster than control mice. In addition, i.v. injection of MSCs and intradermal injection of SLC/CCL21 together further encouraged wound repair. These data suggest that MSCs contribute to wound repair by differentiating into multiple skin cell types. Furthermore, SLC accelerated wound closure of MSCs injected-mice in a dose-dependent manner (Fig. 4*G*).

We showed that circulating MSC was recruited by SLC/CCL21. Furthermore, SLC/CCL21 accelerated MSCs accumulation in wound site, especially the formation endothelial transdifferentiated cells. For that reason, we speculated that SLC/CCL21 may enhance differentiation of MSCs into endothelial cells. To investigate endothelial differentiation of MSC was enhanced by SLC/CCL21, we cultured MSCs in endothelial cell differentiation medium containing SLC/CCL21. CD31 positive cells were presumed to identify MSC transdifferentiated endothelial cells. The number of endothelial cell was no difference between SLC/CCL21 added and not added (data not shown).

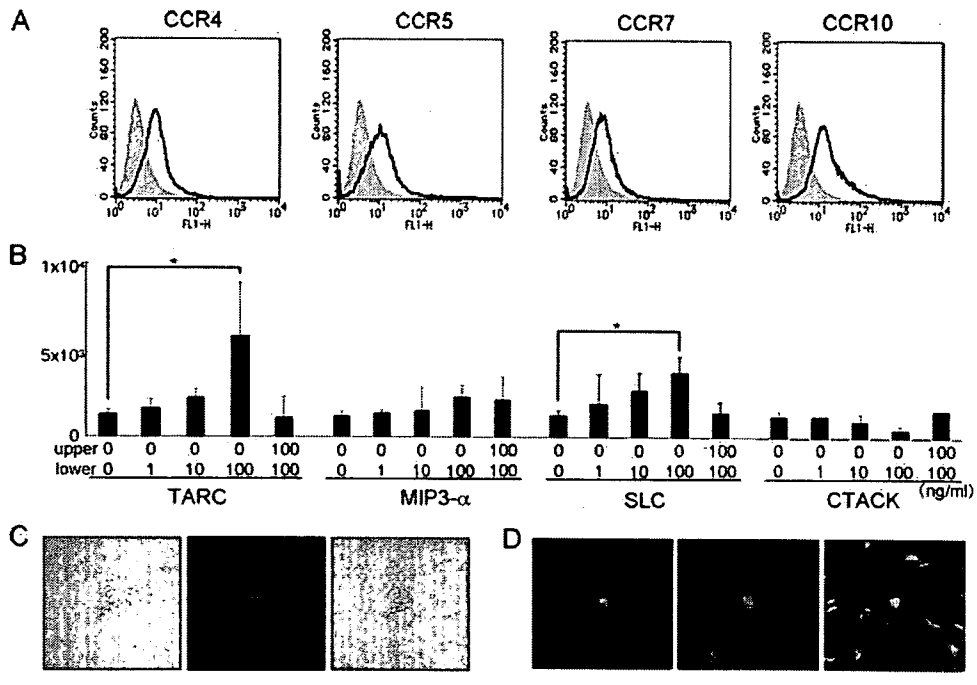

FIGURE 3. MSCs are recruited by specific chemokin/chemokine receptor interactions. *A*, Chemokine receptor expression on MSCs were analyzed by flow cytometry. Staining with a specific Ab for each chemokine receptor (solid line) and the background staining with the nonspecific Ig Ab (negative isotype matched control; shaded profile). *B*, Chemotaxis assays were undertaken in vitro. MSCs were added to the upper well of a 8-μm pore Transwell chamber. Indicated recombinant chemokines were added to the upper and/or lower plate. MSCs migration rates increased in response to medium containing recombinant SLC/CCL21 or TARC (*, $p < 0.05$) vs medium alone ($n = 4$). *C*, Migrated MSCs induced by SLC/CCL21 in chemotaxis assay were positive of CCR7 expression. *D*, In wound site of MSC injected mice, GFP positive cells (green) were colocalized with CCR7 (red). Nuclear staining was blue.

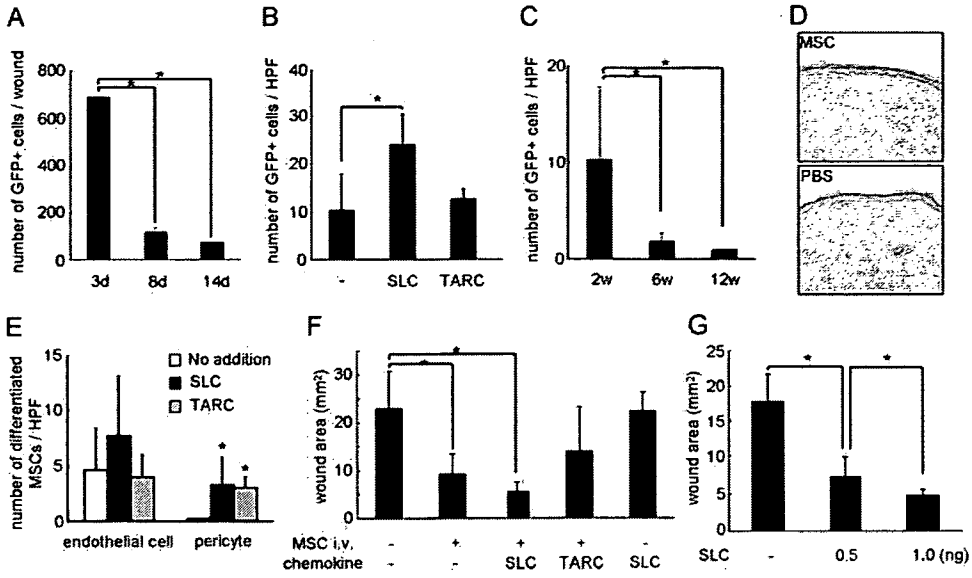

FIGURE 4. MSCs are recruited into wounded skin and contribute to wound repair. *A*, The number of MSCs accumulated into wounded sites was analyzed by flow cytometry (*, $p < 0.05$). *B*, The number of MSCs in wounded sites with local application of 3 μg of chemokine (SLC/CCL21 or TARC) was counted in the HPF (*, $p < 0.05$). Time course analysis of the number of MSCs (2, 6, and 12 wk) (*C*), and the number of MSC-differentiated endothelial cells and pericytes (*E*) were also counted (*, $p < 0.05$). *D*, H&E staining of healed skin of MSC injected mice and that of PBS-injected mice at 15 days after full-thickness cutaneous injury. *F*, Wound size was measured at 8 days after injury and subsequent chemokine treatment (total 3 μg in 100 μl) or PBS (100 μl) as control (5 mice in each group). Intradermal injection of SLC/CCL21 significantly accelerated wound closure (*, $p < 0.05$). *G*, SLC accelerated wound closure of MSCs injected-mice in a dose-dependent manner (*, $p < 0.05$).

Discussion

In this article, we showed that MSCs may come to express keratin 14, keratinocyte marker, in vitro. In wounds, we also showed that MSCs have the capacity to differentiate into multiple skin cell types including keratinocytes, endothelial cells, pericytes, and monocytes. Furthermore, circulating MSC recruitment was induced by a specific chemokine (SLC/CCL21)/chemokine receptor (CCR7) interaction both in vitro and in vivo. Intradermal injection of SLC/CCL21 significantly accelerated wound closure by increasing rates of MSC accumulation, especially the formation of endothelial transdifferentiated cells.

In wound healing process, inflammation is very important phenomenon because inflammation process including induction of inflammatory factors and accumulation of various inflammatory cells. Inflammatory factors and inflammatory cells start tissue regeneration by replenishment of cells and extracellular components. We previously reported that SLC/CCL21 was expressed in keratinocytes of wounded skin (31). Taken together, stimulated keratinocytes produce SLC/CCL21 and MSCs are accumulated in wound site, then contribute wound repair by transdifferentiation into multiple skin cell types.

Several clinical trials using MSCs have been attempted, including for the treatment of neurological diseases (17), spinal injury (16), and myocardial infarction (15). Although several reports have proved some efficacy for MSCs, it is still controversial whether MSCs can contribute significantly to regenerate damaged tissue via tissue specific transdifferentiation. This may be explained, at least in part, by poor viability of the transplanted cells. Furthermore, a suitable microenvironment to promote specific transdifferentiation might be strictly provided, so that MSCs local application without additional treatment failed to form a biologically complete tissue. Physiological accumulation of enough MSCs might induce further cell type differentiation, resulting in better functional organization of the wounded tissue. Although the transdifferentiation mechanism of MSCs has been vigorously investigated, it has not attained a sufficient level that can be used in clinical applications. Accumulation of circulating MSCs, predominantly delivered from bone marrow stroma to the specific tissue might be one of the efficient strategy for tissue regeneration. In our study, 7.4×10^2 MSC were detected in the wound skin of MSC injected mouse (1×10^6 i.v.). Recent paper (32) reported that injected MSCs (1×10^6 i.v.) were detected predominantly in blood (5×10^4) and lungs (5×10^4) and relatively low numbers of MSCs were detected in femoral bone marrow (1×10^2), spleen (1×10^4), liver (2×10^3), and brain (5×10^2). These data indicate that the transplanted MSCs circulate in the blood and are capable of extravasating into tissue. It seems to be reasonable that 6.9×10^2 MSC were detected in 1 × 1 cm wounded skin in our experiment (1×10^6 MSC were injected).

There are still questions about origin and multipotentiality of MSCs. MSCs can be considered nonhemopoietic multipotent stem-like cells that are capable of differentiating into both mesenchymal and nonmesenchymal lineages (33). However, there is no specific single marker to clearly define MSCs. In fact, at present, MSCs are identified through a combination of physical, phenotypic, and functional properties. The classical assay used to identify MSCs is the colony forming unit assay that identifies adherent spindle shaped cells that proliferate to form colonies and can be induced to differentiate into adipocytes, osteocytes, and chondrocytes (33). Because MSC in our study qualify this criteria, we used the term "mesenchymal stem cells" in this article. Furthermore, it is still questionable whether MSCs from bone marrow differentiate into keratinocytes in normal wound repair. From present data, we showed that injected-MSCs contribute to wound repair via accumulation in wound site. In addition, it has been reported that MSCs circulate in normal state (19). However, it is difficult to label resident MSC because there is no specific single marker to clearly define MSCs. Further studies should prove MSCs has true stem cell potential.

If the marker for the keratinocyte-transdifferentiating MSCs is found, we can enrich them by the marker and transdifferentiate